Recognition of Oscillatory Ships in Missile-Borne SAR

*SUN Bing, YANG Ziyue, ZHI Yihang, LIU Yanqing, MEN Zhirong**

School of Electronic and Information Engineering, Beihang University, Beijing 100191, P. R. China

(Received 1 July 2025; revised 19 August 2025; accepted 21 August 2025)

Abstract: An end-to-end recognition strategy is proposed for oscillatory ships in missile-borne synthetic aperture radar (SAR), eliminating the need for image refocusing. Unlike conventional "focus-then-recognize" paradigm, the approach directly exploits oscillation-degraded SAR images for training and recognition, avoiding the unreliability of refocusing under complex imaging conditions. A multi-azimuth ship dataset under the "sea state five" condition is simulated, where ResNet-18 achieves a baseline accuracy of 66.66%, validating the feasibility of the end-to-end framework. By further incorporating a domain-adversarial neural network (DANN) to extract cross-azimuth invariant features, the recognition rate increases to 76.22%, demonstrating the potential of this strategy. The results indicate that, even with a non-optimal backbone, the end-to-end approach shows clear applicability in challenging scenarios, while offering a foundation for future performance gains with more advanced architectures.

Key words: synthetic aperture radar (SAR); oscillatory ship recognition; end-to-end; domain adaptation

CLC number: TN925 **Document code:** A **Article ID:** 1005-1120(2025)04-0477-10

0 Introduction

Ships serve as essential carriers in the global maritime transportation system, playing an irreplaceable strategic role in resource exploitation[1], economic exchange[2], and national security[3]. As marine development continues to grow in scope and depth, application scenarios such as maritime surveillance and tactical early warning place increasing demands on real-time and accurate ship target monitoring[4-5].

Imaging radar systems can acquire high-resolution two-dimensional images of targets over long distances, providing essential information for subsequent target detection and recognition. To meet the specific demands of modern maritime missions, synthetic aperture radars (SARs) have become a key sensing modality for ship monitoring and recognition, owing to their advantages of all-weather, all-day imaging capabilities and high resolution[6-8]. Consequently, SAR image-based ship recognition technologies have become a focus of research in the fields of marine remote sensing and maritime management.

Motion is both the foundation of imaging and the root of its problems[9]. SAR systems acquire images based on the relative motion between the platform and the target. However, maritime ships experience wave-induced, multi-degree-of-freedom motions with strong nonlinearity, which cause significant interference with SAR imaging and result in severe defocusing. Under complex sea conditions, large-amplitude ship motions can lead to substantial image distortion, ultimately degrading recognition performance.

Many researchers have investigated the impact of ship oscillations on SAR imaging. Wang et al.[10] systematically studied the spatially and temporally varying defocus characteristics induced by ship oscillation. Zhou et al.[11] conducted quantitative analysis on the degradation of SAR image quality caused by ship oscillation. In terms of SAR image refocusing, Wang et al.[12] proposed a three-dimensional refocusing method for oscillatory ships based on spatially

*Corresponding author, E-mail address: menzhirong@buaa.edu.cn.

How to cite this article: SUN Bing, YANG Ziyue, ZHI Yihang, et al. Recognition of oscillatory ships in missile-borne SAR [J]. Transactions of Nanjing University of Aeronautics and Astronautics, 2025, 42(4): 477-486.

http://dx.doi.org/10.16356/j.1005-1120.2025.04.004

variant defocus characteristics, effectively enhancing image quality and enabling ship recognition under severe defocus conditions. Guo et al.[13] presented a coarse-to-fine refocusing approach for maneuvering ship targets in spaceborne SAR, combining ISAR techniques with high-order spatial motion compensation to mitigate residual defocus and improve image clarity. While these methods demonstrate considerable potential, refocusing remains highly challenging for ships undergoing complex motions in missile-borne and large-squint SAR scenarios. In the field of SAR image-based ship recognition, most recent research has leveraged deep learning methods. Zhang[14] proposed a classification method based on multi-convolutional neural network fusion to address the low recognition accuracy of small and medium-sized ships; nevertheless, it does not fully account for the image degradation induced by ship oscillation and its potential constraints on recognition performance. Zhang et al.[15] conducted a systematic study on ship oscillation recognition from both real-valued and complex-valued perspectives and proposed an enhanced refocusing method to improve the recognition accuracy of oscillatory ship targets.

Recognizing oscillatory ships in missile-borne SAR systems faces several challenges. Unlike airborne and spaceborne platforms, missile-borne SAR presents additional difficulties. (1) There is a lack of publicly available and high-quality datasets. The high maneuverability and complex imaging geometry of missile-borne platforms[16], combined with military sensitivity and security issues, hinder the collection and sharing of real-scene data covering diverse ship motions and attitude changes. Most existing public SAR datasets are limited to spaceborne or airborne platforms, which significantly restricts the usefulness and generalization of data-driven approaches and deep learning models. (2) Large squint angles cause significant range-Doppler coupling and nonlinear imaging geometry. Coupled with defocusing due to target motion, oscillatory ships may experience notable geometric distortion under these conditions. (3) The short synthetic aperture time limits coherent integration, preventing the capture of an entire oscillation cycle and leading to incomplete motion data, which increases variability within classes.

In addition, the continuously varying attitude of oscillatory ship targets causes image distortion and defocusing, which further complicates recognition[10-11]. Moreover, due to the inherent azimuth sensitivity of SAR imaging[17], targets of the same class may appear significantly different under varying initial heading directions, leading to category confusion or recognition failure[18]. Conventional recognition methods usually depend on image refocusing as a preprocessing step. However, in the current application scenario, such refocusing is highly challenging and might even be ineffective. Additionally, in real-world processing pipelines, the amount of information content can at most be preserved and cannot be increased; inappropriate preprocessing might cause the loss of discriminative features, thereby degrading recognition performance. To explore a better processing approach, this study adopts an end-to-end strategy, enabling the network to automatically learn feature representations and effectively mitigate the information loss caused by manual preprocessing.

To address these challenges, a simulated dataset of oscillatory ships was created by selecting three ship types and covering all heading directions. For recognition, the ResNet-18 network was initially used to run experiments on the simulated dataset, providing preliminary validation of the feasibility of the end-to-end strategy in this scenario. To further mitigate azimuth sensitivity, a domain adaptation strategy was introduced to enhance the cross-domain generalization. Specifically, the domain-adversarial neural network (DANN) was integrated with ResNet-18 to form the overall architecture. The feasibility and limitations of the proposed scenario were analyzed through experiments, demonstrating the significant potential of the end-to-end strategy for performance improvement.

1 SAR Imaging Modeling

1.1 Ship oscillation

The attitude disturbance of a ship under wave

action can be approximated as a three-degree-of-freedom rigid-body rotation about its center of mass, namely pitch, roll, and yaw, as shown in Fig. 1. Under real sea states, these rotational motions are governed by a complex coupling of wave excitation, buoyant restoring forces, and added mass effects, making the motion modeling highly complex.

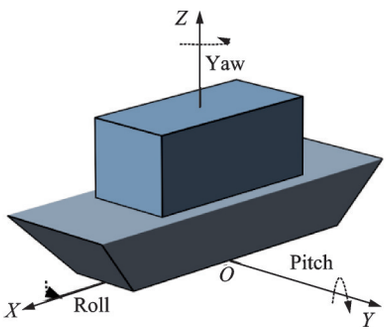

Fig.1 Ship oscillation model

In imaging simulation studies, the angular displacement in each rotational degree of freedom can be approximated by a sinusoidal function[19], and the instantaneous rotation angle of the ship at time t can thus be expressed as

$$\theta_{\mathrm{p}}(t)=\frac{1}{2}A_{\mathrm{p}}\sin\left(\frac{2\pi}{T_{\mathrm{p}}}t+\varphi_{\mathrm{p}}\right) \tag{1}$$

$$\theta_{\mathrm{y}}(t)=\frac{1}{2}A_{\mathrm{y}}\sin\left(\frac{2\pi}{T_{\mathrm{y}}}t+\varphi_{\mathrm{y}}\right) \tag{2}$$

$$\theta_{\mathrm{r}}(t)=\frac{1}{2}A_{\mathrm{r}}\sin\left(\frac{2\pi}{T_{\mathrm{r}}}t+\varphi_{\mathrm{r}}\right) \tag{3}$$

where $\theta_{\mathrm{p}}(t)$, $\theta_{\mathrm{y}}(t)$, and $\theta_{\mathrm{r}}(t)$ are the rotating angles of the pitch, yaw, and roll, respectively; A_{p}, A_{y}, and A_{r} the double amplitudes of the pitch, yaw, and roll, respectively; T_{p}, T_{y}, and T_{r} the motion periods of the pitch, yaw, and roll, respectively; φ_{p}, φ_{y}, and φ_{r} the initial phase offsets of the pitch, yaw, and roll, respectively.

To transform the physical model into a mathematical formulation, a local coordinate system is established concerning the ship's body axes to describe its absolute motion. As shown in Fig.1, the origin is set at the center of the keel, with the longitudinal axis defined as the x-axis, the transverse axis as the y-axis, and the vertical axis as the z-axis. In this local frame, (X_P, Y_P, Z_P) denotes the position of a scattering point P on the ship. Using a rotating matrix, its coordinates in the global coordinate system can be expressed as (x_P, y_P, z_P), shown as

$$\begin{bmatrix}x_P\\y_P\\z_P\end{bmatrix}=\mathbf{Rot}(\theta_x,\theta_y,\theta_z)\begin{bmatrix}X_P\\Y_P\\Z_P\end{bmatrix} \tag{4}$$

where the rotating matrix **Rot** is derived through the ordered multiplication of yaw, pitch and row[20]. The individual roll oscillation matrices $\mathbf{Rot}_{\mathrm{y}}$, $\mathbf{Rot}_{\mathrm{p}}$, and $\mathbf{Rot}_{\mathrm{r}}$ can be expressed as

$$\mathbf{Rot}=\mathbf{Rot}_{\mathrm{r}}\cdot\mathbf{Rot}_{\mathrm{p}}\cdot\mathbf{Rot}_{\mathrm{y}} \tag{5}$$

$$\mathbf{Rot}_{\mathrm{y}}=\begin{bmatrix}\cos\theta_{\mathrm{y}}(t) & -\sin\theta_{\mathrm{y}}(t) & 0\\ \sin\theta_{\mathrm{y}}(t) & \cos\theta_{\mathrm{r}}(t) & 0\\ 0 & 0 & 1\end{bmatrix} \tag{6}$$

$$\mathbf{Rot}_{\mathrm{p}}=\begin{bmatrix}\cos\theta_{\mathrm{p}}(t) & 0 & \sin\theta_{\mathrm{p}}(t)\\ 0 & 1 & 0\\ -\sin\theta_{\mathrm{p}}(t) & 0 & \cos\theta_{\mathrm{p}}(t)\end{bmatrix} \tag{7}$$

$$\mathbf{Rot}_{\mathrm{r}}=\begin{bmatrix}1 & 0 & 0\\ 0 & \cos\theta_{\mathrm{r}}(t) & -\sin\theta_{\mathrm{r}}(t)\\ 0 & \sin\theta_{\mathrm{r}}(t) & \cos\theta_{\mathrm{r}}(t)\end{bmatrix} \tag{8}$$

1.2 Echo signal in missile-borne SAR

In the missile-borne SAR imaging model, the radar platform is assumed to fly at a constant altitude with a constant velocity and fixed flight direction. The transmitted signal is a linear frequency modulated (LFM) pulse, whose two-dimensional time-domain expression is given by[9]

$$S_{\mathrm{t}}(\tau,t)=\mathrm{rect}\left[\frac{\tau}{T_{\mathrm{p}}}\right]\exp\left\{\mathrm{j}2\pi\left(f_{\mathrm{c}}t+\frac{1}{2}K\tau^2\right)\right\} \tag{9}$$

where f_{c} is the carrier frequency, T_{p} the pulse duration, and K the chirp rate. t and τ denote the azimuth slow time and range fast time, respectively. After reflection and down conversion at the receiver, the echo phase can be written as

$$\phi_{\mathrm{r}}(\tau,t)=\exp\left(-\mathrm{j}\frac{4\pi f_{\mathrm{c}}R_{\mathrm{s}}}{c}\right)\exp\left[\mathrm{j}\pi K\left(\tau-\frac{2R_{\mathrm{s}}^2}{c}\right)\right] \tag{10}$$

where R_{s} is the one-way slant range. Denoting the radar platform coordinates as $(x_{\mathrm{r}}, y_{\mathrm{r}}, z_{\mathrm{r}})$, R_{s} between a scattering point P on the ship and the radar can be expressed as

$$R_{\mathrm{s}}(\tau)=\sqrt{(x_{\mathrm{r}}-x_{\mathrm{p}})^2+(y_{\mathrm{r}}-y_{\mathrm{p}})^2+(z_{\mathrm{r}}-z_{\mathrm{p}})^2} \tag{11}$$

Ship oscillation induces scattering point displacement, causing slant range R_s deviation. It introduces phase errors in the echo described by Eq.(11), leading to matched filter mismatch and image defocusing, thereby degrading recognition performance.

2 Dataset Construction

To construct a remote sensing image dataset for ship recognition tasks, three representative ship types are chosen and named Class A, Class B, and Class C in this paper. These ships share certain similarities in size and shape, allowing for a more objective assessment of recognition algorithm performance.

To simulate ship oscillation, a relatively harsh sea state, sea state five, is selected. For oscillation amplitude and period parameters, typical values in Table 1 are used as means, with random sampling within specified ranges to enhance data diversity and realism. The initial azimuth angle for each ship class is uniformly distributed over 0°—360° to capture imaging variations across different heading directions. Some sample examples are shown in Fig.2.

Table 1 Oscillation parameters at sea state 5[19]

Level	Motion	Amplitude/(°)	Period/s
Sea state five	Pitch	3.4	6.7
	Yaw	3.8	14.2
	Roll	38.4	12.2

The fidelity of simulations is essential for any study. However, due to the scarcity of publicly available real-world data for this scenario, it remains difficult to quantitatively compare simulated and measured samples. To improve the realism of the simulation, the ship's structure was modeled with electromagnetic software to generate the radar cross-section (RCS) data. Motion imaging simulations were then conducted based on typical ship motion parameters from Ref.[19]. During imaging, the ship's attitude was recorded at 0.06 ms intervals, generating SAR images that closely match the actual results. The back projection (BP) algorithm was employed for imaging simulation. For each ship type, 360 SAR image samples were generated, totaling 1 080 samples.

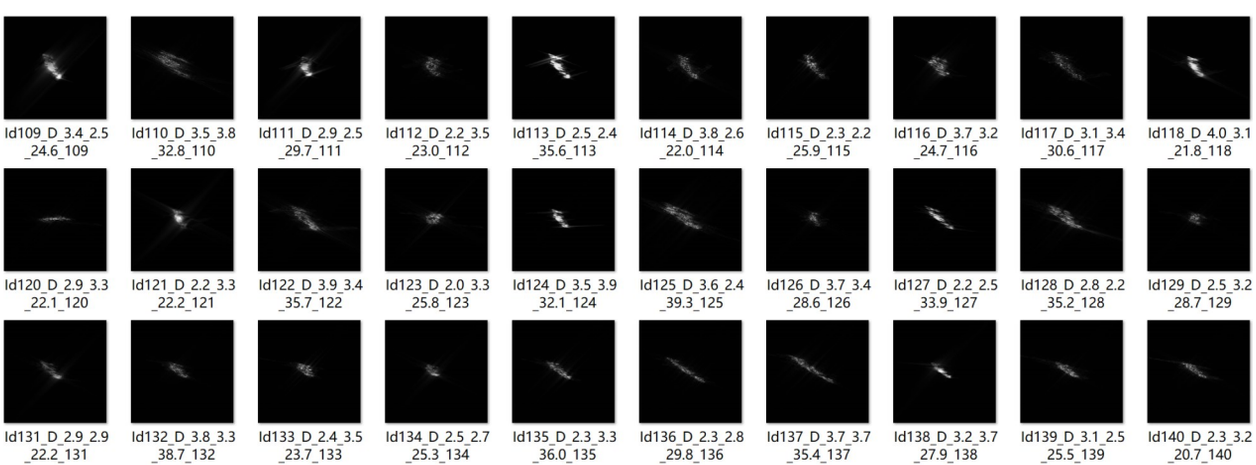

Fig.2 Sample examples from the dataset

3 Recognition of Oscillatory Ships in ResNet-18

3.1 ResNet-18 network architecture

ResNet introduces residual connections that effectively alleviate gradient vanishing and performance degradation in deeper networks, enabling stable deep feature learning and prime recognition performance[21]. Compared to deeper ResNet variants, ResNet-18 feature fewer parameters and lower computational cost, offering enhanced training stability and robustness against overfitting in SAR image scenarios with limited samples and significant target

scale variations. Its shallower structure also preserves low-level texture and contour details, which is critical for recognizing targets with blurred structures and indistinct edges in SAR imagery. Moreover, it has demonstrated solid performance in previous SAR image recognition studies. Hence, ResNet-18 is selected as the backbone network in this paper.

The ResNet-18 architecture in Table 2[21] consists of four residual stages, each containing two 3×3 convolutions followed by batch normalization and ReLU for better nonlinearity and stability. It starts with a 7×7 convolution and max pooling, then moves through progressively deeper layers to extract multi-scale features. It concludes with global average pooling and a fully connected layer (FC) for recognition. FC-*C* denotes FC with the output dimension of *C*.

Table 2 Architecture of the ResNet-18 network[21]

Module	Output size	Parameter	Stride
Conv 1	64×128×128	7×7 conv	2×2
Max pooling	64×64×64	3×3 max pool	2×2
Conv 2	64×64×64	$\begin{bmatrix}3\times3\text{ conv}\\3\times3\text{ conv}\end{bmatrix}\times2$	1×1
Conv 3	128×32×32	$\begin{bmatrix}3\times3\text{ conv}\\3\times3\text{ conv}\end{bmatrix}\times2$	2×2
Conv 4	256×16×16	$\begin{bmatrix}3\times3\text{ conv}\\3\times3\text{ conv}\end{bmatrix}\times2$	2×2
Conv 5	512×8×8	$\begin{bmatrix}3\times3\text{ conv}\\3\times3\text{ conv}\end{bmatrix}\times2$	2×2
Average pooling	512×1×1	2×2	1×1
FC-*C*	*C*×1	*C*	
Softmax	*C*×1	*C*	

3.2 Model training

The dataset was randomly split into training, validation, and test sets in an 8∶1∶1 ratio. ResNet-18 served as the backbone network and was trained for 800 epochs. Model performance was tracked through validation accuracy and training loss. As shown in Fig.3, the recognition accuracy steadily improves as training continues. Although there was instability in the early stages, the performance eventually converged to about 65% after sufficient training. Fig.4 shows a consistent decrease in loss, highlighting the effectiveness of continued training. After 500 epochs, the loss curve begins to level off, indicating convergence.

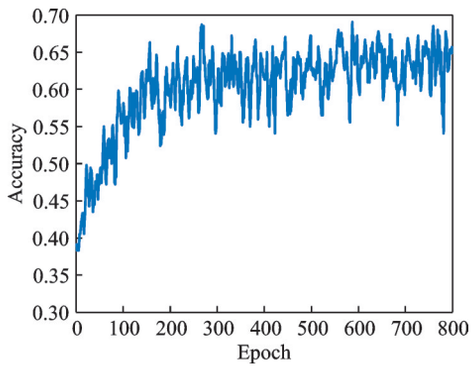

Fig.3 Validation accuracy during training

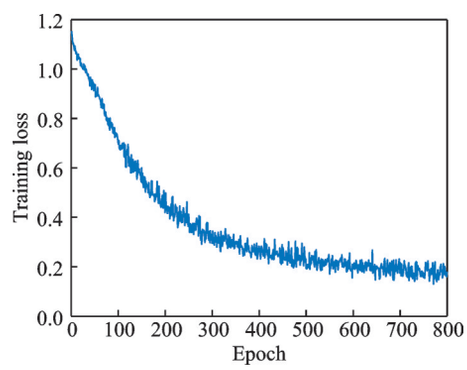

Fig.4 Training loss during training

3.3 Model evaluation

Table 3 gives the per-class recognition accuracy and the corresponding confusion matrices. The model attains an overall accuracy of 66.66%.

Table 3 Recognition accuracy and confusion matrix of ResNet-18

Class	Confusion matrix			Recognition accuracy/%
	Class A	Class B	Class C	
A	28	0	8	77.78
B	4	19	13	52.78
C	4	5	25	69.44

Analysis of the results reveals marked class-wise imbalance and randomness in recognition rates. Under the "sea state five" condition, the pronounced ship oscillation induces strong SAR defocus and structural distortion, sharply reducing both feature extraction effectiveness and feature expressiveness. Therefore, under more challenging sea states, the performance of existing recognition schemes may degrade significantly or even collapse entirely. Nevertheless, on the present dataset, ResNet-18 exhibits a degree of recognition capability and maintains an acceptable accuracy level, preliminarily demonstrating the feasibility of the end-to-end strategy.

4 Recognition of Oscillatory Ships in Domain Adaptive

4.1 Domain adaptation strategy

This study uses an end-to-end recognition strategy that avoids complex image refocusing or preprocessing. However, distortions and significant azimuth sensitivity still exist in SAR imagery. To alleviate the azimuth sensitivity issue, transfer learning is applied in hopes of improving recognition accuracy in this challenging scenario.

Dataset analysis indicates that, in missile-borne SAR large squint-angle imaging, ship oscillations induce pronounced defocus and distortion. Variations in initial heading directions further alter target orientation and introduce diverse distortions, resulting in substantial intra-class variability. This variability impedes effective feature sharing and reduces model robustness and generalization. To enhance recognition, the model must extract class-consistent representations across azimuths while reducing azimuth-induced discrepancies.

Based on this observation, a domain adaptation strategy is employed. The dataset is divided into a labeled source domain and an unlabeled target domain via random azimuth-based splitting. Discriminative features are learned from the source domain through supervised learning, while adversarial learning aligns feature distributions across domains to extract domain-invariant representations[22]. This approach enhances recognition accuracy for unseen azimuths and enables effective classification of target domain samples. ResNet-18 is adopted as the backbone network and integrated into the DANN architecture. The complete framework is shown in Fig.5.

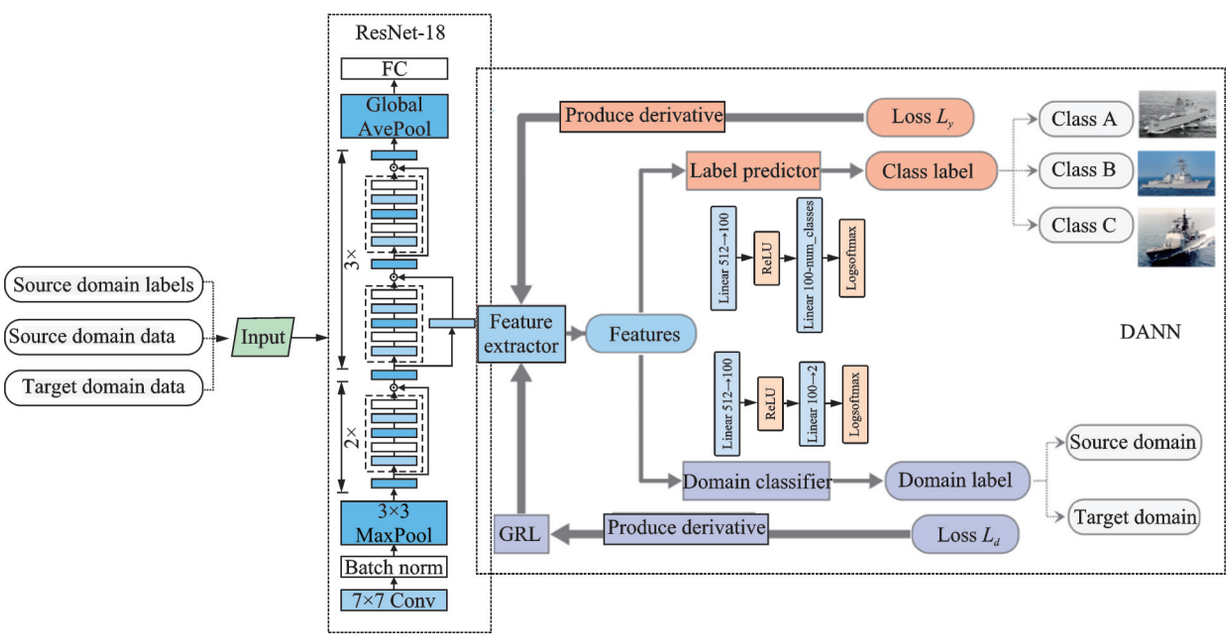

Fig.5 DANN-based ResNet-18 framework

4.2 DANN network architecture

DANN is a classic domain adaptation framework[23] widely applied in cross-domain image classification, medical imaging, speech recognition, and sentiment analysis[24]. As shown in Fig.5, the architecture comprises three key components: Feature extractor, label predictor, and domain classifier.

The feature extractor captures high-level features to distinguish ship categories. The label predictor, a supervised subnetwork of fully connected layers, takes these features and predicts categories for source-domain samples, providing supervision. Training involves forward propagation, loss evaluation, gradient backpropagation, and parameter updates via Adam optimizer for robust source domain performance. The domain classifier processes features through fully connected layers with nonlinear

activations to make domain predictions, serving as the core of adversarial learning.

A gradient reversal layer (GRL) is inserted between the extractor and classifier to reverse gradients during backpropagation, enabling the extractor to generate domain-agnostic features and align feature distributions. To balance early classification with later domain adaptation, a dynamic coefficient alpha is integrated into the GRL, gradually increasing from 0 to 1 following a sigmoid schedule. This allows the model to initially focus on classification and then shift to domain alignment, enhancing training stability and effectiveness.

4.3 Model training and result analysis

In this study, an unsupervised domain adaptation method was employed. The target domain data were treated as samples with unknown categories, and their labels were not used during training. This approach guarantees that improvements in classification performance truly reflect the model's ability to generalize, rather than label leakage. It also simulates a real-world scenario in which the target domain remains unlabeled, a situation frequently encountered in missile-borne SAR applications, where the acquisition of labeled data is often costly or infeasible.

The dataset was randomly split into source and target domains in an 8∶2 ratio. The model was trained for 800 epochs. To monitor convergence and assess recognition performance on both domains, class-wise recognition accuracy on the target domain was recorded at each epoch. Analysis of the results shows fluctuating performance in the early training phases. As training continues, recognition accuracy gradually stabilizes. The results suggest that the model's performance converges after about 400 epochs, with the overall recognition rate settling at around 77%. Once stabilized, the target-domain recognition accuracy averages 76.22%.

The legends in Fig.6 are as follows: Target domain-All, Target domain-Class A, Target domain-Class B, and Target domain-Class C, which respectively represent the recognition accuracy variations during training for all target domain samples, and target domain ships of Class A, Class B, and Class C.

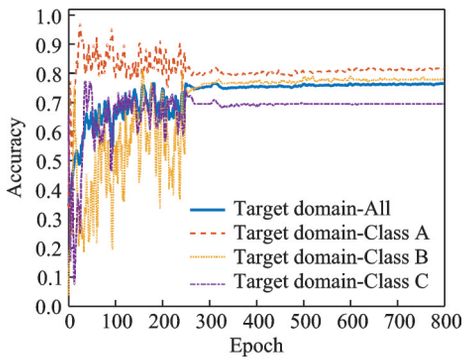

Fig.6 Recognition accuracy under sea state five conditions

In this study, the discrepancy in total sample counts between Tables 3 and 4 is due to the dataset partitioning strategy, which depends on the network architecture. For ResNet-18, a validation subset was used during training, resulting in 108 images in the test set (Table 3). Conversely, the DANN network did not require a validation set, and 216 images were used for evaluation (Table 4). The confusion matrix and per-class recognition rates from a representative epoch of the DANN network are shown in Table 4.

Table 4 Recognition accuracy and confusion matrix of DANN

Class	Confusion matrix			Recognition accuracy/%
	Class A	Class B	Class C	
A	58	11	3	80.55
B	3	56	13	77.77
C	12	10	50	69.44

The results indicate that domain adaptation significantly improves target-domain recognition, as well as convergence speed and training stability. This benefit comes from using unlabeled target data in adversarial training, which guides the model toward learning transferable, class-discriminative features and makes better use of labeled source data. However, its effectiveness might decrease in more challenging conditions. Overall, the efficacy and applicability of DANN in this scenario are confirmed, further demonstrating the feasibility and potential of the end-to-end strategy in this application, based on the ResNet-18 backbone.

Furthermore, obvious limitations are present. DANN heavily relies on the target domain distribution: Its adversarial loss promotes feature represen-

tations closely aligned with the target data, so the resulting model achieves high accuracy only within that target domain or similar distributions. When test data differ significantly from the target distribution, the model's effectiveness drops substantially. Therefore, although domain adversarial training can greatly enhance recognition in a specific domain, its wider applicability remains limited and needs further improvement.

It should be noted that no direct comparison with existing state-of-the-art recognition algorithms was performed. However, a few of the prior studies have specifically targeted this application scenario, which is characterized by multi-azimuth sensitivity and scattering distortions under large squint angles. Moreover, this work aims to experimentally validate the feasibility of end-to-end recognition and its potential performance gains in complex imaging conditions. ResNet-18 was selected as the baseline network due to its strong performance in prior SAR target recognition studies, providing a reference for improvements and enabling a more objective and practical assessment of performance gains. Future work will systematically compare newly available algorithms with the proposed method to achieve comprehensive cross-method evaluation and further verify the applicability of end-to-end recognition in complex SAR scenarios.

5 Conclusions

This paper focuses on the recognition of oscillatory ships in missile-borne SAR imagery, i.e., a scenario marked by significant azimuth sensitivity and notable image distortion and defocus caused by target oscillation. To directly address these challenges, we propose an end-to-end recognition framework that skips traditional preprocessing methods such as image refocusing or deblurring, thereby testing the viability of data-driven approaches in challenging imaging conditions.

Firstly, a comprehensive SAR dataset covering a full range of ship heading directions has been created. This dataset captures the azimuth-induced appearance variability inherent to missile-borne SAR, effectively simulating the recognition challenges encountered in real-world deployments. Our observations reveal that, under large squint angles, The ship oscillation leads to severe defocus and distortion. Moreover, variations in initial ship heading induce distinct geometric deformations, resulting in substantial intra-class appearance differences for the same target.

Regarding recognition performance, an end-to-end strategy was implemented, directly excluding complex image preprocessing procedures. Initial experiments employing ResNet-18 under the "sea state five" condition revealed considerable performance declines, highlighting the challenges of ship recognition in scenarios involving severe motion-induced image distortions, while also demonstrating the feasibility of the end-to-end strategy. To counteract the azimuth sensitivity, DANN was subsequently integrated with the ResNet-18 feature extraction module. Through adversarial learning, the model acquired class-discriminative yet heading-invariant feature representations, resulting in a notable 9.56% improvement in recognition accuracy. This progress substantiates the effectiveness of transfer learning methods, particularly domain-adversarial techniques, in alleviating appearance variations caused by significant heading changes in missile-borne SAR imagery, thereby confirming the practicality and potential of the end-to-end strategy for recognition in complex SAR imaging conditions.

Lastly, this study reveals that while the DANN-based strategy significantly improves cross-heading recognition, its effectiveness is highly domain-dependent. The learned features exhibit strong correlation with the target domain data, which limits its generalization when the test domain deviates substantially from the training distribution. These findings emphasize the need for more robust domain adaptation strategies in real-world SAR recognition tasks. Overall, the end-to-end recognition strategy shows significant potential for performance gains and practical application, with future integration of more advanced network architectures expected to

boost recognition results even more.

References

[1] KALUZA P, KÖLZSCH A, GASTNER M T, et al. The complex network of global cargo ship movements[J]. Journal of the Royal Society Interface, 2010, 7(48): 1093-1103.

[2] HOFFMANN J, WILMSMEIER G, LUN Y H V. Connecting the world through global shipping networks[J]. Journal of Shipping and Trade, 2017, 2: 1-4.

[3] XU M, PAN Q, XIA H, et al. Estimating international trade status of countries from global liner shipping networks[J]. Royal Society Open Science, 2020, 7(10): 200386.

[4] TIWARI S P, CHATURVEDI S K, ADHIKARY S, et al. Automatized marine vessel monitoring from Sentinel-1 data using convolution neural network[C]// Proceedings of the 2021 IEEE International Geoscience and Remote Sensing Symposium IGARSS. [S. l.]: IEEE, 2021.

[5] SOLDI G, GAGLIONE D, FORTI N, et al. Space-based global maritime surveillance. Part Ⅰ: Satellite technologies[J]. IEEE Aerospace and Electronic Systems Magazine, 2021, 36(9): 8-28.

[6] ZHANG M, CHEN Y, LYU X, et al. Synthetic aperture radar ship detection in complex scenes based on multifeature fusion network[J]. Journal of Applied Remote Sensing, 2023, 17(1): 016511.

[7] MARGARIT G, BARBA MILANÉS J A, TABASCO A. Operational ship monitoring system based on synthetic aperture radar processing[J]. Remote Sensing, 2009, 1(3): 375-392.

[8] RIZAEV I G, KARAKUŞ O, HOGAN S J, et al. Modeling and SAR imaging of the sea surface: A review of the state-of-the-art with simulations[J]. ISPRS Journal of Photogrammetry and Remote Sensing, 2022, 187: 120-140.

[9] CUMMING I G, WONG F H. Digital processing of synthetic aperture radar data[J]. Boston: Artech House, 2005.

[10] WANG J, LENG X, SUN Z, et al. Study of space / time varying defocus characteristics of complex moving ship targets in SAR imaging[J]. Systems Engineering and Electronics, 2024, 46(7): 2237-2255.

[11] ZHOU B, QI X, ZHANG J, et al. Effect of six-DOF rotation of ship target on SAR imaging[J]. IEEE Journal of Selected Topics in Applied Earth Observations and Remote Sensing, 2021, 14(5): 1621-1634.

[12] WANG J, LENG X, SUN Z, et al. Refocusing swing ships in SAR imagery based on spatial-variant defocusing property[J]. Remote Sensing, 2023, 15 (12): 3159.

[13] GUO J, YANG W, CHEN J, et al. Refocusing of moving ship targets in SAR images with long synthetic aperture time[C]//Proceedings of the IGARSS 2022 IEEE International Geoscience and Remote Sensing Symposium. [S.l.]: IEEE, 2022.

[14] ZHANG Xiao. Research on ship detection and classification in SAR images[D]. Harbin: Harbin Institute of Technology, 2020. (in Chinese)

[15] ZHANG Yun, HUA Qinglong, JIANG Yicheng, et al. Recognition of 3D oscillatory ship targets based on mixed complex-valued convolutional neural network[J]. Acta Electronica Sinica, 2022, 50 (5): 1042-1049. (in Chinese)

[16] BAO M, ZHOU S, XING M. Processing missile-borne SAR data by using cartesian factorized back projection algorithm integrated with data-driven motion compensation[J]. Remote Sensing, 2021, 13(8): 1462.

[17] GE J, WANG C, ZHANG B, et al. Azimuth sensitive object detection of high-resolution SAR images in complex scenes by using a spatial orientation attention enhancement network[J]. Remote Sensing, 2022, 14 (9): 2198.

[18] DING B, WEN G, HUANG X, et al. Target recognition in SAR images by exploiting the azimuth sensitivity[J]. Remote Sensing Letters, 2017, 8(8): 821-830.

[19] WEHNER D R. High resolution radar[M]. Norwood, MA: Artech House, 1987.

[20] ARDAKANI H A, BRIDGES T J. Review of the 3-2-1 euler angles: A yaw-pitch-roll sequence[EB/OL]. (2025-03-04). http://personalpages. surrey. ac. uk/t. bridges/SLOSH/3-2-1-Eulerangles. pdf.

[21] HE K, ZHANG X, REN S, et al. Deep residual learning for image recognition[C]//Proceedings of the IEEE Conference on Computer Vision and Pattern Recognition. [S.l.]: IEEE, 2016.

[22] LI J J, YU Z Q, DU Z K, et al. A comprehensive survey on source-free domain adaptation[J]. IEEE Transactions on Pattern Analysis and Machine Intelligence, 2024, 46(8): 5743-5762.

[23] GANIN Y, USTINOVA E, AJAKAN H, et al. Domain adversarial training of neural networks[J]. Journal of Machine Learning Research, 2016, 17(59): 1-35.

[24] CAI X, WU Z, ZHONG K, et al. Unsupervised cross-lingual speech emotion recognition using domain adversarial neural network[C]//Proceedings of the 2021 12th International Symposium on Chinese Spo-

ken Language Processing (ISCSLP). [S.l.]: IEEE, 2021.

Authors

The first author Prof. **SUN Bing** received his B.S. and Ph. D. degrees from Beihang University, Beijing, China, in 2003 and 2008, respectively. He became a Lecturer, after finishing his postdoctoral research, Beihang University, in 2010. He was a visiting scholar with The University of Texas-Pan American, Edinburg, TX, USA, from November 2013 to November 2014. He has been a professor with Beihang University since 2025. His research interests include synthetic aperture radar top-level design and simulation, signal processing and quality evaluation, and pattern recognition.

The corresponding author Dr. **MEN Zhirong** received the B.S. and Ph.D. degrees from Beihang University, Beijing, China, in 2014 and 2018, respectively. From 2018 to 2020, he became a postdoctoral researcher at School of Electronic and Information Engineering, Beihang University. He was a visiting scholar at School of Mathematics and Statistics, University of Sheffield, UK, from 2019 to 2020. He is currently an associate professor at Beihang University. His research interests include advanced microwave imaging radar systems, imaging signal processing, and ionospheric effect analysis and mitigation.

Author contributions Prof. **SUN Bing** conceptualized the study, provided the research process, and revised the manuscript. Miss. **YANG Ziyue** conducted the literature review, compiled the models, performed the analysis, interpreted the results, and wrote the manuscript. Mr. **ZHI Yihang** contributed to data processing and assisted in the analysis. Mr. **LIU Yanqing** helped improve the experimental design and participated in the revision of the manuscript. Dr. **MEN Zhirong** provided guidance on SAR imaging methodologies and offered critical revisions to enhance the technical accuracy of the manuscript. All authors commented on the manuscript draft and approved the submission.

Competing interests The authors declare no competing interests.

(Production Editor: SUN Jing)

弹载SAR图像晃动舰船识别

孙 兵，杨子悦，植一航，刘艳青，门志荣

(北京航空航天大学电子信息工程学院，北京 100191，中国)

摘要：提出了一种面向弹载合成孔径雷达(Synthetic aperture radar，SAR)晃动舰船的端到端识别方法。不同于传统的“先聚焦再识别”范式，所提方法直接利用散焦畸变的SAR图像进行训练与识别，从而避免复杂成像条件下再聚焦过程的复杂性与不可靠性。本文构建了5级海况条件下的多方位舰船数据集，基线实验结果表明，ResNet-18模型能够实现66.66%的识别精度，验证了端到端框架的可行性。在此基础上，引入领域对抗神经网络(Domain-adversarial neural network，DANN)以提取方位不变特征，识别率提升至76.22%，验证了端到端框架的识别性能提升潜力。实验结果表明，即便所采用的主干网络并非最优，端到端方法在该应用场景下仍能展现出良好的适用性，为结合更先进的网络结构以进一步提升端到端策略的识别性能奠定基础。

关键词：合成孔径雷达；晃动舰船识别；端到端；域自适应